

## Influence of reduction mechanism on the morphology of cobalt nanoparticles in a silica-gel matrix

A. Basumallick

Department of Metallurgical Engineering, Bengal Engineering College (D.U.),  
Howrah-711 103, India

G.C. Das and S. Mukherjee

Department of Metallurgical Engineering, Jadavpur University, Calcutta-700 032, India

(Received 16 June 1999; accepted 7 October 1999)

Cobalt-chloride- and dextrose-containing silica gels were reduced *in situ* under nitrogen atmosphere in the temperature range of 600 to 950 °C. Analysis of kinetic data on the *in situ* reduction shows that, in the temperature range of 600 to 750 °C, the contracting geometry type and, in the temperature range of 800 to 950 °C, the nucleation and growth type of mechanisms remain operative. The shape and size of the reduced cobalt nanoparticles in the silica matrix was studied by examining the transmission electron micrographs of the reduced Co/SiO<sub>2</sub> samples. The morphology of the reduced metallic particles was found to be influenced by the change in reduction mechanism.

### I. INTRODUCTION

During the last few years preparation of glass-metal nanocomposites via the sol-gel route has gained considerable importance.<sup>1-5</sup> This new class of materials exhibits remarkable electrical<sup>2,3,6</sup> and magnetic<sup>7</sup> properties, which has raised the possibility of their commercial exploitation as substrates for semiconduction technology.<sup>8</sup> The shape and size of the nanoparticles present in the host matrix influence the physical properties to a great extent. However, it has been reported that the shape and size of the metallic islands in the host matrix vary within wide limits.<sup>9</sup> Such wide deviation in shape and size imparts a great deal of inconsistency in the results of physical characterization of these novel materials. Therefore, we feel strongly that, unless the physical properties are tailored to be uniform through precise control of shape and size, the possibility of commercial exploitation of these materials appears to be eclipsed. Control over the morphology of the particles from the fundamental viewpoint can be achieved by controlling the kinetic parameters and thereby by the mechanism(s) of conversion of gels to nanocomposites. Considering the above views in the backdrop, the present paper reports the effect of kinetic parameters, e.g., temperature and time, and conversion mechanism(s) on the morphology of CoCl<sub>2</sub>-containing SiO<sub>2</sub> gels reduced to Co-SiO<sub>2</sub> nanocomposites.

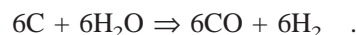
### II. EXPERIMENTAL

SiO<sub>2</sub> gels containing CoCl<sub>2</sub> and a stoichiometric amount of dextrose as reductant were prepared by using a sol containing tetraethyl orthosilicate (TEOS)

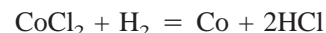
and CoCl<sub>2</sub> in ethyl alcohol. The volume ratio of C<sub>2</sub>H<sub>5</sub>OH:TEOS was maintained at 4:1 for all the gel samples. The detailed preparation technique has been described elsewhere.<sup>9</sup> The resulting gels were then subjected to isothermal reduction treatment in the temperature range 600 to 950 °C at an interval of 50 °C under N<sub>2</sub> atmosphere. The N<sub>2</sub> flow rate was maintained at 5 cc/s throughout the experiment. The reduction treatments were carried out in an electrical heating furnace. The desired temperature was maintained by a PID controller with an accuracy of ±1 °C. The heat treatment led to the decomposition of dextrose:



which subsequently generated H<sub>2</sub> *in situ*:



The H<sub>2</sub> so generated *in situ* reduced CoCl<sub>2</sub> at the sites.



The HCl vapor generated during the course of the heat treatment is absorbed in a known volume of double-distilled water. The pH values of the resulting HCl solution were recorded as a function of heat-treatment time. The pH values of the solution yield [H<sup>+</sup>] in the solution from which the fraction of CoCl<sub>2</sub> reduced was calculated. The gels on complete reduction would yield 5 wt% Co/SiO<sub>2</sub> nanocomposite.

### III. RESULTS AND DISCUSSION

The effect of time and temperature on the *in situ* isothermal reduction of CoCl<sub>2</sub>-containing gel samples in the temperature ranges 600 to 750 °C and 800 to 950 °C are

shown separately in Fig. 1 and Fig. 2, respectively, since the reduction characteristics and mechanisms are conspicuously different from each other in the above mentioned temperature ranges.

The appropriate reaction mechanism(s) which remain operative during the course of reduction has been identified by analyzing experimental kinetic data on time-dependent fractional conversion through reduced time analysis. The analysis is as follows. The general equation<sup>10</sup> for a particular mechanism is written as

$$g(\alpha) = kt \quad (1)$$

where  $g(\alpha)$  is an appropriate function of fractional conversion  $\alpha$ ,  $t$  is the time, and  $k$  is the specific rate constant which depends on the type of mechanism(s).

For  $\alpha = n$ ,

$$g(n) = kt_n \quad (2)$$

where  $t_n$  is the time required for fractional conversion of  $n$ .

Dividing Eq. (1) by Eq. (2), we get

$$g(\alpha)/g(n) = t/t_n = \theta \quad (3)$$

where  $\theta$  is the reduced time. Equation (3) is independent of  $k$ , the reaction rate constant, which is the temperature-dependent term in kinetics. Therefore, for the same mechanism operative over the entire range of temperature, the computed  $\alpha$  versus  $\theta$  plot from experimental data will coincide with the theoretically computed  $\alpha$  versus  $\theta$  plot for the mechanism(s). By comparing the computed  $\alpha$  versus  $\theta$  plot for the mechanisms, it is possible to

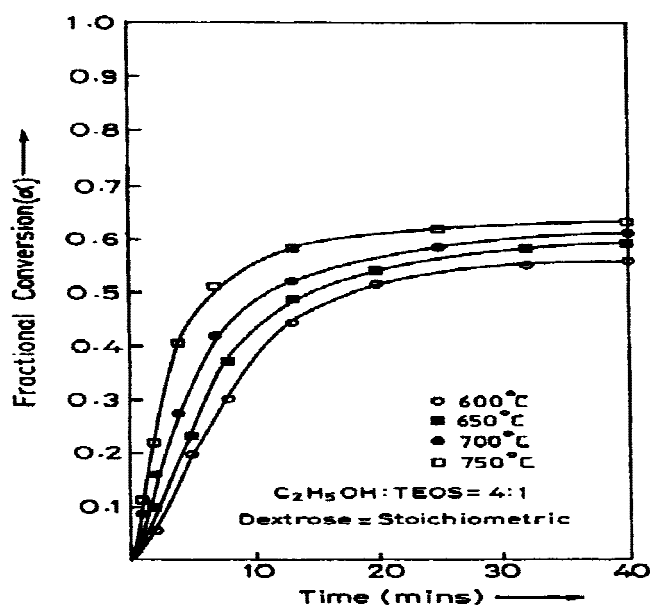


FIG. 1. Fractional conversion ( $\alpha$ ) versus time ( $t$ ) plots of the isothermal *in situ* reduction of  $\text{CoCl}_2$ -containing  $\text{SiO}_2$  gels in the temperature range of 600 to 750 °C.

find out the mechanism which remains actually operative. The list of relevant mechanisms along with the form of  $g(\alpha)$  and symbols is shown in Table I.

The reduced time plots corresponding to Figs. 1 and 2 are shown in Figs. 3 and 4, respectively. It is evident from Fig. 3 that in the low-temperature range the contracting geometry (CG3) type of mechanism remains operative in the initial stages of reduction which changes to a diffusion-controlled mechanism (D1, D3, or D4) at higher fractional conversion. The change of mechanism has been observed to occur above a value of  $\alpha = 0.45$ . Therefore, suitable values of  $\alpha \geq 0.45$  were selected over which the reduced time analysis has been done separately. The dotted lines in the reduced time plot (Fig. 3)

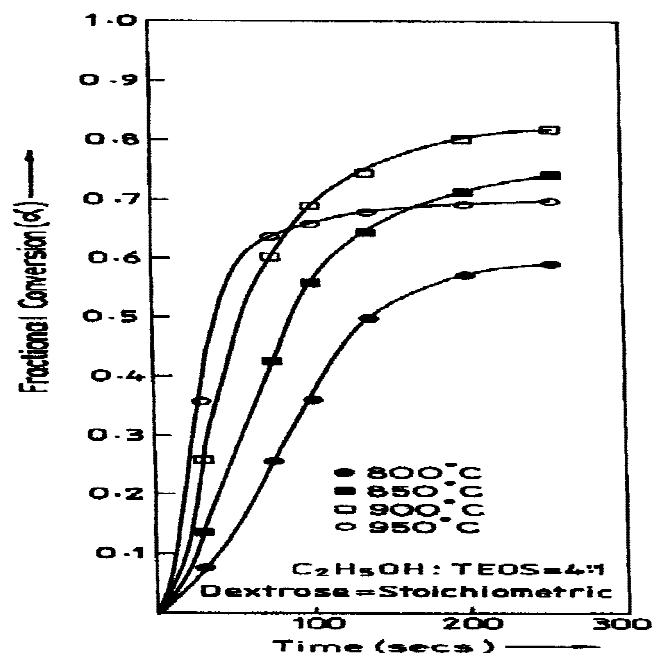


FIG. 2. Fractional conversion ( $\alpha$ ) versus time ( $t$ ) plots of the isothermal *in situ* reduction of  $\text{CoCl}_2$ -containing  $\text{SiO}_2$  gels in the temperature range of 800 to 950 °C.

TABLE I. Mechanisms of gas–solid reactions.

Name	Symbol	Form of $g(\alpha) = kt$
Diffusion-controlled type		
Parabolic	D1	$\alpha^2 = kt$
Valensi Barrer	D2	$\alpha + (1 - \alpha) \ln(1 - \alpha) = kt$
Ginstling Brounhtein	D3	$1 - 2/3\alpha - (1 - \alpha)^{2/3} = kt$
Jander	D4	$[1 - (1 - \alpha)^{1/3}]^2 = kt$
Contracting Geometry type		
Linear	CG1	$\alpha = kt$
Cylindrical symmetry	CG2	$1 - (1 - \alpha)^{1/2} = kt$
Spherical symmetry	CG3	$1 - (1 - \alpha)^{1/3} = kt$
Nucleation and growth type		
Avrami Erofeev $n = 1.5$	NG1	$[-\ln(1 - \alpha)]^{1/1.5} = kt$
Avrami Erofeev $n = 2.0$	NG2	$[-\ln(1 - \alpha)]^{1/2.0} = kt$
Avrami Erofeev $n = 3.0$	NG3	$[-\ln(1 - \alpha)]^{1/3.0} = kt$

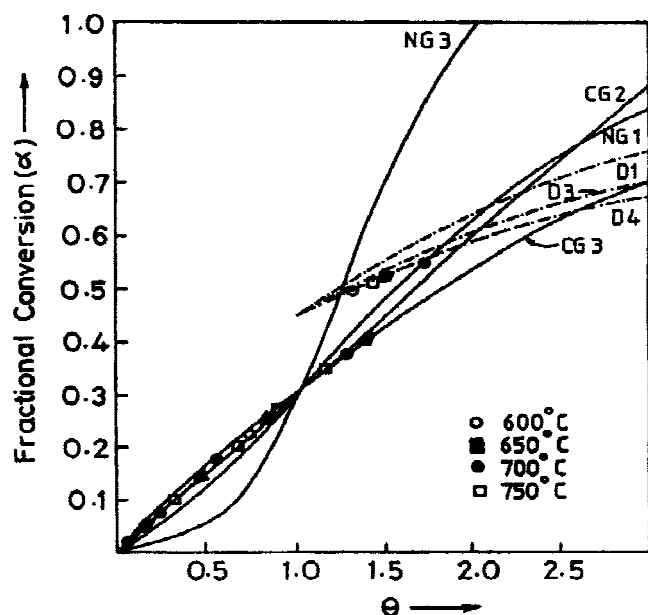


FIG. 3. Reduced time plot of the isothermal *in situ* reduction of  $\text{CoCl}_2$ -containing  $\text{SiO}_2$  gels in the temperature range of 600 to 750 °C.

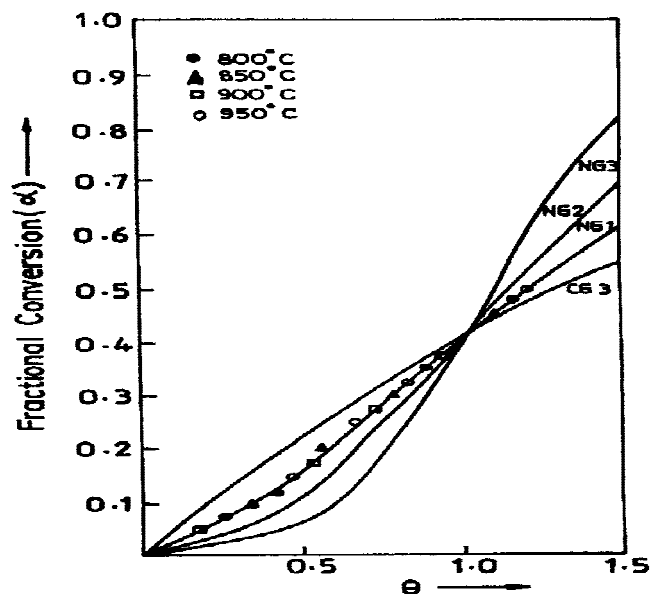
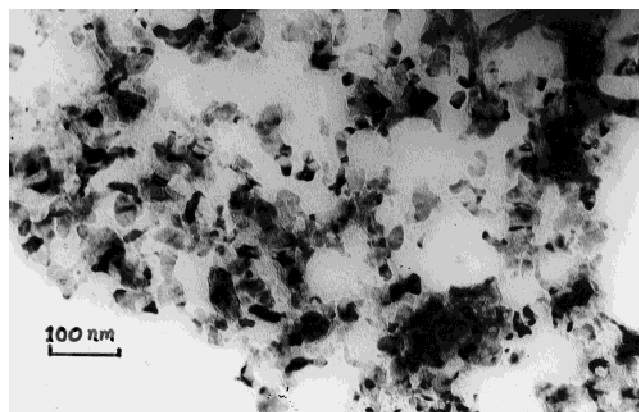


FIG. 4. Reduced time plot of the isothermal *in situ* reduction of  $\text{CoCl}_2$ -containing  $\text{SiO}_2$  gels in the temperature range of 800 to 950 °C.

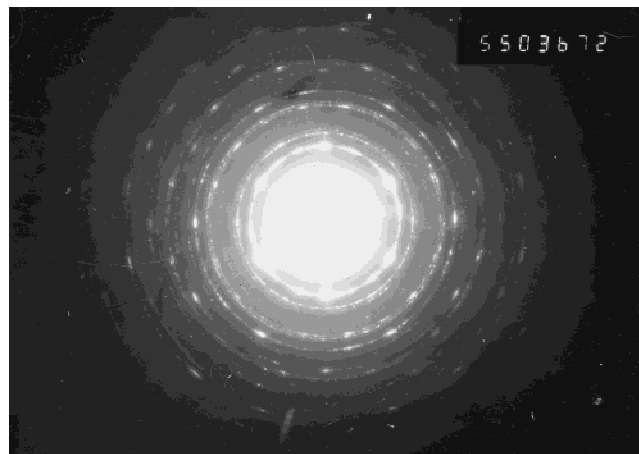
represent the superimposed reduced time plots for  $\theta = t/t_{0.45}$ . The analysis has been done separately due to the following reasons. According to the reduced time analysis,  $g(\alpha_1)/g(\alpha_2) = k_1 t/k_2 t_m$ , where  $\alpha_1$  and  $\alpha_2$  are the fractional conversion at times  $t$  and  $t_m$ , respectively. It is worth mentioning that  $k_1$  and  $k_2$  will be equal only when the mechanism remains isokinetic at a particular temperature in the time span of  $t$  to  $t_m$ . Therefore, if it does not remain isokinetic, the related mechanism cannot be identified accurately.

The validity of the operating mechanisms can be established on the basis of the fact that the vapor pressure of  $\text{CoCl}_2$  in the temperature range 600 to 700 °C is negligibly small<sup>11</sup> and the reduction occurs only between the *in situ* generated  $\text{H}_2$  and solid  $\text{CoCl}_2$  particles present in the nanosized interconnected pores of the  $\text{SiO}_2$  gels. Therefore, similar to other gas–solid reactions it is quite logical that the reduction mechanism will depend significantly on the initial geometry of the  $\text{CoCl}_2$  particles. Initially, a thin layer of metallic Co will be formed over the  $\text{CoCl}_2$  particles which come in contact with the *in situ* generated  $\text{H}_2$ . Further, reduction will occur at the Co/ $\text{CoCl}_2$  interface by the diffusion of  $\text{H}_2$  at the reaction interface which will move toward the center.

Figures 5(a) and 6(a) represent the transmission electron photographs of the nanocomposites reduced at 650 and 750 °C, respectively. It is clearly evident from the photographs that the nanosized Co particles embedded in the  $\text{SiO}_2$  matrix possess either cylindrical or spherical shape, and the sharpness in their contours has been observed to decrease appreciably with increase in tempera-

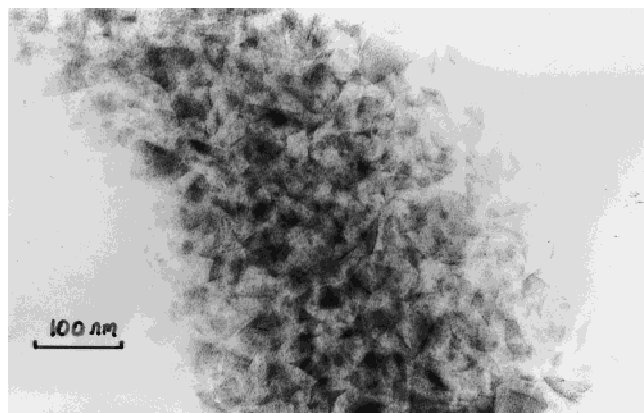


(a)



(b)

FIG. 5. (a) TEM photograph of the  $\text{CoCl}_2$ -containing  $\text{SiO}_2$  gel sample reduced at 650 °C. (b) Corresponding SAD pattern.



(a)



(b)

FIG. 6. (a) TEM photograph of the  $\text{CoCl}_2$ -containing  $\text{SiO}_2$  gel sample reduced at  $750^\circ\text{C}$ . (b) Corresponding SAD pattern.

ture. This has been attributed to the insipient fusion of unreduced  $\text{CoCl}_2$  in the  $\text{Co-CoCl}_2$  mixture. The above observations are direct evidence of the fact that the reduction mechanism is dependent on the initial geometry of the  $\text{CoCl}_2$  particles and is of contracting geometry type. The presence of Co particles in the matrix has been confirmed by computing the  $d_{hkl}$  values from the corresponding selected-area diffraction (SAD) pattern shown in Figs. 5(b) and 6(b), respectively. The computed  $d_{hkl}$  values have been found to match reasonably well with the ASTM  $d_{hkl}$  values of Co.

In the later stage of reduction, the adsorbed water vapor becomes exhausted and the  $\text{H}_2$  gas generated at this stage is only through the water vapor available from the polycondensation of the  $\text{SiO}_2$  gel. The polycondensation reaction being sluggish in nature tends to lower  $\text{H}_2$  gas generation and subsequently lowers the availability of  $\text{H}_2$  at the reaction interface, which in turn lowers the overall gas–solid reaction and the rate of fractional conversion. The above effects causes the change in mechanism from contracting geometry to diffusion-controlled type.

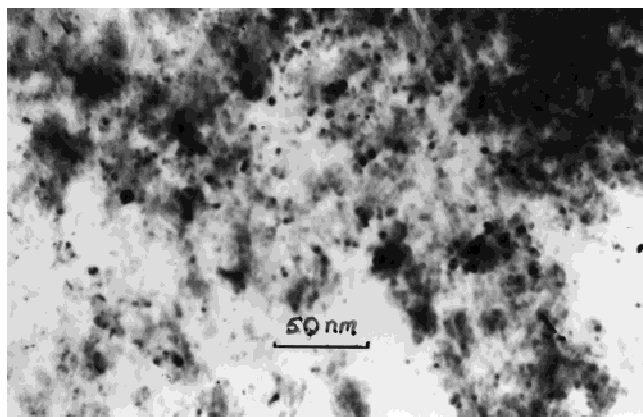
In the temperature range of  $800$  to  $900^\circ\text{C}$  the reduced time plot (Fig. 4) clearly indicates that the nucleation and growth (NG) type of mechanism remains operative as compared to the operative contracting geometry (CG) type of mechanism in the lower temperature range. The validity of the nucleation and growth type of mechanism can be physically established by taking recourse to the fact that the equilibrium vapor pressure of  $\text{CoCl}_2$  rises sharply in the range of  $800$  to  $950^\circ\text{C}$ .<sup>11</sup> Therefore, it is highly probable that the *in situ* generated  $\text{H}_2$  will reduce  $\text{CoCl}_2$  in the vapor state. Since the melting point of Co is very high ( $1480^\circ\text{C}$ ), solid Co particles will precipitate out from the vapor phase by a nucleation and growth process. However, conversion of  $\text{CoCl}_2$  to metallic Co in the gaseous state will decrease the vapor pressure of  $\text{CoCl}_2$ . Therefore, to maintain the equilibrium vapor pressure,  $\text{CoCl}_2$  will be vaporized continuously. Since the reduction in the gaseous phase is much faster than the gas–solid or gas–liquid reaction, nucleation and growth of Co from the vapor state will control the kinetics of reduction. The amount of Co precipitation and the growth of fine Co particles on increasing the reduction temperature have been clearly revealed in the TEM photograph. Therefore, the nucleation and growth type of mechanism is physically viable.

Figures 7(a) and 8(a) represent the TEM micrographs of the reduced gel samples at  $850$  and  $950^\circ\text{C}$ . On examination of the micrographs carefully, an agglomeration of very fine spherical particles, which possess features similar to those of the particles deposited from the gaseous phase,<sup>12</sup> can be observed. It is also observed that with the increase in temperature the deposition of metallic Co particles from the gaseous phase increases and the fine particles deposited initially grow in size by particle coarsening. The particles deposited at the initial stages act as nuclei for further deposition. Therefore, this observation corroborates the fact that the nucleation and growth type mechanism remains operative. Figures 7(b) and 8(b) represent the corresponding SAD pattern in this temperature range. The  $d_{hkl}$  values computed from the SAD pattern have been again found to match reasonably well with the ASTM standard  $d_{hkl}$  values of Co.

#### IV. CONCLUSIONS

The conclusions which are drawn from the present study are as follows.

(1) During the *in situ* reduction of  $\text{CoCl}_2$  in the silica-gel matrix in the temperature range of  $600$  to  $750^\circ\text{C}$ , the contracting geometry type of mechanism remains operative in the initial stages which changes to the diffusion-controlled type of mechanism at higher fractional conversion.

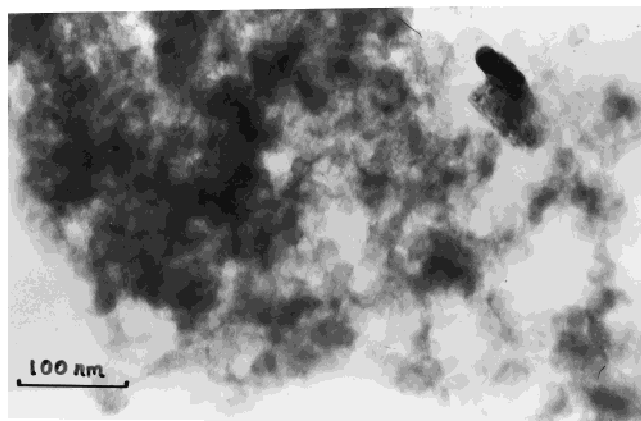


(a)

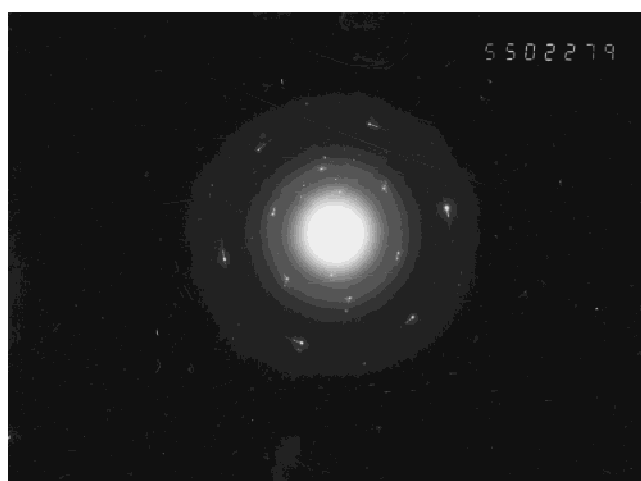


(b)

FIG. 7. (a) TEM photograph of the  $\text{CoCl}_2$ -containing  $\text{SiO}_2$  gel sample reduced at 850 °C. (b) Corresponding SAD pattern.



(a)



(b)

FIG. 8. (a) TEM photograph of the  $\text{CoCl}_2$ -containing  $\text{SiO}_2$  gel sample reduced at 950 °C. (b) Corresponding SAD pattern.

(2) The operating *in situ* reduction mechanism in the temperature range of 800 to 950 °C is markedly different from the operating mechanism at 600–750 °C and has been found to be of nucleation and growth type.

(3) In the low-temperature range the initial geometry of the  $\text{CoCl}_2$  particles present in the silica matrix exerts a significant influence on the shape and size of the reduced metallic particles. At the onset of the reaction, a thin layer of Co is formed over the  $\text{CoCl}_2$  particles. Further reduction occurs at the Co/ $\text{CoCl}_2$  interface by the diffusion of *in situ* generated  $\text{H}_2$  to the interface.

(4) The nanosized reduced Co particles present in the host matrix possess a mixture of cylindrical and spherical shapes in the temperature range of 600 to 750 °C.

(5) In the temperature range of 800 to 950 °C *in situ* reduction of  $\text{CoCl}_2$  by  $\text{H}_2$  occurs in the gaseous phase. Very fine metallic particles which bear the characteristics of precipitation from the gaseous phase have been observed. The rate of precipitation as well as growth of fine particles has been observed to increase with the increase in reduction temperature.

## REFERENCES

1. A. Chatterjee and D. Chakravorty, *J. Phys. D: Appl. Phys.* **22**, 1386 (1989).
2. A. Chatterjee and D. Chakravorty, *J. Phys. D: Appl. Phys.* **23**, 1097 (1990).
3. D. Chakravorty, *Bull. Mater. Sci.* **15**, 411 (1992).
4. K. Susa, I. Matsuyama, S. Satoh, and T. Suganama, *J. Non-Cryst. Solids* **119**, 21 (1990).
5. A. Basumallick, K. Biswas, G.C. Das, and S. Mukherjee, *J. Mater. Res.* **10**, 2938 (1995).
6. A. Chatterjee and D. Chakravorty, *J. Mater. Sci.* **27**, 4115 (1992).
7. W. Gong, H. Li, Z. Zhao, and J. Chen, *J. Appl. Phys.* **69**, 5119 (1991).
8. T. Mori, M. Toki, M. Ikejiri, M. Taker, M. Aoki, S. Uchiyama, and S. Kanbe, *J. Non-Cryst. Solids* **100**, 523 (1988).
9. A. Basumallick, K. Biswas, S. Mukherjee, and G.C. Das, *J. Mater. Lett.* **30**, 363 (1997).
10. J.H. Sharp, G.W. Brindley, and B.N. Achar Narahaki, *J. Am. Ceram. Soc.* **49**, 379 (1966).
11. R.H. Perry and C.H. Chilton, in *Chemical Engineer's Handbook* (Kogakusha Ltd, Tokyo, 1983), pp. 3–46.
12. G.W. Nieman, J.R. Weertman, and R.W. Siegel in *Clusters and Cluster-Assembled Materials*, edited by R.S. Averbach, J. Bernholc, and D.L. Nelson (*Mater. Res. Soc. Symp. Proc.* **206**, Pittsburgh, PA, 1991), p. 493.